0026-895X/07/7105-1277–1287$20.00
MOLECULAR PHARMACOLOGY
Copyright © 2007 The American Society for Pharmacology and Experimental Therapeutics
Mol Pharmacol 71:1277–1287, 2007

Vol. 71, No. 5
33563/3201688
Printed in U.S.A.

Insulin Increases the Potency of Glycine at Ionotropic Glycine Receptors

Valerie B. Caraiscos, Robert P. Bonin, J. Glen Newell, Elzbieta Czerwinska, John F. Macdonald, and Beverley A. Orser

Institute of Medical Science (V.B.C., B.A.O.), Departments of Physiology (R.P.B., J.F.M., E.C., B.A.O.) and Anesthesia (B.A.O.), Sunnybrook Health Sciences Centre, University of Toronto, Toronto, Ontario, Canada

Received December 22, 2006; accepted February 15, 2007

ABSTRACT

The mechanisms by which insulin modulates neuronal plasticity and pain processes remain poorly understood. Here we report that insulin rapidly increases the function of glycine receptors in murine spinal neurons and recombinant human glycine receptors expressed in human embryonic kidney cells. Whole-cell patch-clamp recordings showed that insulin reversibly enhanced current evoked by exogenous glycine and increased the amplitude of spontaneous glycinergic miniature inhibitory postsynaptic currents recorded in cultured spinal neurons. Insulin (1 μM) also shifted the glycine concentration-response plot to the left and reduced the glycine EC_{50} value from 52 to 31 μM. Currents evoked by a submaximal concentration of glycine were increased to approximately 140% of control. The glycine receptor α subunit was sufficient for the enhancement by insulin because currents from recombinant homomeric α_1 receptors and heteromeric $\alpha_1\beta$ receptors were both increased. Insulin acted at the insulin receptor via pathways dependent on tyrosine kinase and phosphatidylinositol 3 kinase because the insulin effect was eliminated by the insulin receptor antagonist, hydroxy-2-naphthalenylmethylphosphonic acid trisacetoxymethyl ester, the tyrosine kinase inhibitor lavendustin A, and the phosphatidylinositol 3 kinase antagonist wortmannin. Together, these results show that insulin has a novel regulatory action on the potency of glycine for ionotropic glycine receptors.

Insulin has been studied extensively as a regulator of metabolic processes; however, its role in regulating neuronal transmission has only recently been explored. Insulin diffuses into the central nervous system from peripheral sources and is also produced in the brain, in which it binds to cell surface receptors and activates a variety of signaling molecules (Schulingkamp et al., 2000). Neurons can secrete insulin in a calcium-dependent manner when depolarized (Clarke et al., 1986). Furthermore, insulin receptors and their substrates are widely expressed in the brain and spinal cord. In particular, insulin receptors are predominantly located in laminas V and X of the spinal cord, which suggests involvement in sensory pathways (Sugimoto et al., 2002). Clinical disorders resulting from a deficiency of insulin, such as diabetes mellitus, are characterized by neuropathic pain (Park, 2001). The short-term administration of insulin reduces the concentration of inhaled anesthetic that is required to prevent movement in response to a painful stimulus in a rat model (Xing et al., 2004). This short-term anesthetic-sparing effect of insulin is independent of effects on the concentration of blood glucose. The molecular basis for the analgesic properties and alterations in neurotransmission by insulin has not been elucidated.

Glycine receptors (GlyRs) are the major sites of fast synaptic inhibition in the spinal cord and brainstem (Lynch, 2004). GlyRs in neurons are pentameric complexes assembled from two classes of subunits (α_{1-4}, β), which combine to form chloride (Cl^-)-selective ion channels. The α subunit carries a binding site for both agonists and antagonists and forms fully functional homomeric receptors. The β subunit forms functional channels only when coassembled with α subunits. The β subunit plays a critical role in anchoring GlyRs to synapses, altering the gating kinetics and receptor conductance, and determining receptor sensitivity to a vari-

This research is supported by operating grants from the Canadian Institutes of Health Research (to B.A.O.) (MOP-38028), a Career Scientist Award (to B.A.O.), a Canadian Institutes of Health Research doctoral research award (to V.B.C.) (56381) and postdoctoral fellowship award (to J.G.N.) (63508). B.A.O. is a Canada Research Chair in Anesthesia.

B.A.O. serves as a scientific advisor to Merck Sharp and Dohme Inc.

Article, publication date, and citation information can be found at http://molpharm.aspetjournals.org.

doi:10.1124/mol.106.033563.

ABBREVIATIONS: GlyR, glycine receptor; $GABA_A$, γ-aminobutyric acid subtype A; PKC, protein kinase C; PI3, phosphatidylinositol 3; MEM, minimum essential medium; FBS, fetal bovine serum; DIV, days in vitro; HEK, human embryonic kidney; mIPSC, miniature inhibitory postsynaptic current; HNMPA, hydroxyl-2-naphthalenylmethylphosphonic acid trisacetoxymethyl ester; DMSO, dimethyl sulfoxide; PBS, phosphate-buffered saline; I_{Gly}, glycine current; NMDA, *N*-methyl-D-aspartate; IGF, insulin-like growth factor.

ety of pharmacological compounds (Laube et al., 2002). Native GlyRs are known to play fundamental roles in motor and sensory processes, including the coordination of movement and nociception (Legendre, 2001).

Several lines of evidence predict that insulin modifies GlyR function. First, insulin alters the function and surface expression of several members of the evolutionarily conserved superfamily of channels to which GlyRs belong. Insulin increases currents generated by γ-aminobutyric acid subtype A ($GABA_A$) receptors by increasing the number of receptors expressed at the membrane surface (Wan et al., 1997). In addition, the insulin receptor is a member of the family of receptor tyrosine kinases that activates a number of second-messenger systems involving protein kinase C (PKC), nonreceptor tyrosine kinases, and phosphatidylinositol 3 (PI3) kinase (Saltiel and Pessin, 2002). The function of GlyRs is regulated by PKC, for which both enhancement and depression of glycinergic currents have been reported (Legendre, 2001). GlyR function is also up-regulated by the nonreceptor tyrosine kinase c-Src, which increases receptor function possibly via actions on a tyrosine residue at position 413 of the β subunit (Caraiscos et al., 2002). Given these results, we tested the hypothesis that insulin modulates GlyRs. Using electrophysiological and immunoimaging techniques, we showed that insulin up-regulates GlyR function by increasing the potency of glycine in a manner that is dependent on cytosolic signaling pathways involving tyrosine kinases and PI3 kinase.

Materials and Methods

Spinal Cord Cell Cultures. Primary cultures of spinal cord neurons were prepared from embryonic Swiss white mice. In brief, fetal pups (13–14 days in utero) were removed from mice sacrificed by cervical dislocation. The spinal cord of each fetus was collected for plating. Neurons were plated on collagen-coated 35-mm dishes at a density of 1×10^6 and were grown in MEM supplemented with 10% fetal bovine serum (FBS), 10% horse serum (all from Invitrogen, Carlsbad, CA), 25 mM glucose, 26 mM sodium bicarbonate, and 1.4 μM insulin. After 3 to 5 DIV, a 10 μM fluoro-2′-deoxyuridine solution (5 μM uridine and 5 μM 5-fluoro-2′-deoxyuridine) was added to inhibit glial proliferation, and MEM was replaced with the above-mentioned MEM solution lacking FBS. Low-density spinal cord cultures (~3000 cells/cm^2) were also plated on coverslips coated with poly(D-lysine) and grown in serum-free media that did not contain insulin (Neurobasal MEM, B-27, and N-2 supplements; Invitrogen). For the immunostaining experiments, low-density spinal cord cultures were plated on coverslips coated with poly(D-lysine) and grown at a density of approximately 3000 cells/cm^2 in serum-free MEM (Neurobasal MEM, B-27 supplement; Invitrogen). Fluoro-2′-deoxyuridine was added 24 to 48 h after plating. The cultures were maintained at 37°C in a humidified 5% CO_2 atmosphere and fed twice per week. Whole-cell recording and immunostaining experiments were performed 14 days after plating.

Heterologous Expression of Human Recombinant GlyRs and Immunocytochemical Studies. Human embryonic kidney (HEK) 293 cells (Microbix Biosystem Inc., Toronto, ON, Canada) were maintained in a mixture of MEM with Earle's salts and L-glutamine with 10% FBS (Invitrogen) in a humidified atmosphere containing 5% CO_2 at 37°C. Cells were plated onto poly(D-lysine)-coated coverslips or 35-mm culture dishes and transiently transfected with cDNA constructs encoding human GlyR α_1, or α_1, and β subunits (1:1 ratio) using the Lipofectamine 2000 reagent (Invitrogen). Transfection was performed according to the manufacturer's protocol with a total of 2 μg of cDNA per 35-mm culture dish. The cDNA constructs were subcloned into the pBK-CMV NB-200 expression vector and then sequenced in both directions to confirm the correct reading frame. GlyR α_1/pBK-CMV NB-200 or a combination of GlyR α_1/pBK-CMV NB-200 and GlyR β/pBK-CMV NB-200 (ratio 1:1) was used, and transient protein expression was allowed to proceed for 24 h.

Electrophysiology. Spinal neurons were voltage clamped at −60 mV using standard whole-cell patch-clamp techniques. The extracellular solutions were applied to the neurons using a computer-controlled, multibarreled perfusion system with an exchange time of approximately 3 ms (SF-77B; Warner Instruments, Hamden, CT). To monitor access resistance, a voltage step of −10 mV was applied before each application of glycine. The series resistance was approximately 6 to 12 MΩ. If the series resistance changed by more than 20%, the cell was excluded from further analysis. The extracellular solution contained 140 mM NaCl, 1.3 mM $CaCl_2$, 5.4 mM KCl, 2 mM $MgCl_2$, 25 mM HEPES, and 33 mM glucose, with the pH adjusted to 7.4. Tetrodotoxin (300 nM) was added to the extracellular solution to block voltage-sensitive Na^+ channels. The intracellular solution contained 63 mM CsCl, 70 mM CsF, 11 mM EGTA, 1 mM $CaCl_2$, 2 mM $MgCl_2$, 10 mM HEPES, 10 mM tetraethylammonium, and 3.4 mM potassium-ATP, with pH 7.3. Pipettes were prepared using a two-step puller (PP-83; Narishige Scientific Instrument Lab, Tokyo, Japan). For recordings of spontaneous mIPSCs generated by postsynaptic GlyRs, 6-cyano-7-nitro-quinoxaline-2,3-dione (10 μM), 2-amino-4-phosphonovaleric acid (40 μM), and bicuculline methiodide (10 μM) were added to the extracellular solution to inhibit ionotropic glutamate receptors and $GABA_A$ receptors, respectively. Neurons were voltage-clamped at −70 mV and experiments were performed at room temperature (20–22°C). Some experiments were performed using the gramicidin (Sigma-Aldrich Canada, Oakville, ON, Canada) perforated-patch technique (Akaike, 1996). The pipette solution contained 150 mM potassium gluconate and 10 mM HEPES with the pH adjusted to 7.3 using KOH. The osmolarity of the solution was adjusted to 290 to 300 mOsM using sucrose. Gramicidin stock solution (10 mg/ml in methanol) was diluted in the pipette solution to a final concentration of 50 to 100 μg/ml just before the experiment. The tip of the patch pipette was filled with a potassium gluconate gramicidin-free solution then backfilled with the gramicidin-containing solution. A high-resistance (gigaohm) seal was formed between the electrode and the cell membrane by applying gentle suction after the pipette touched the cell. The electrode was voltage-clamped at −60 mV, and membrane perforation was monitored by applying 10-mV hyperpolarizing pulses every 20 s. A perforated patch with an access resistance of less than 30 MΩ was achieved within 30 min of establishing the gigaohm seal.

Stock solutions of insulin (Sigma-Aldrich) were prepared in acidified water (HCl, pH 2). Stock solutions containing $ZnCl_2$ and tricine (both from Sigma-Aldrich) were prepared in water. For experiments that investigated the role of the insulin receptor and second-messenger systems, HNMPA, lavendustin A, lavendustin B (all from Calbiochem, La Jolla, CA), and wortmannin (Sigma-Aldrich) were dissolved in DMSO. All drugs except wortmannin were applied extracellularly; wortmannin was included in the pipette solution. For experiments using HNMPA, glycine-evoked currents were allowed to reach a stable amplitude over 5 s before drugs were applied as described previously (Caraiscos et al., 2002).

Glycinergic mIPSCs were recorded in the presence of tetrodotoxin and analyzed with Mini Analysis software (Synaptosoft, Decatur, GA). For detection, the detection threshold was set approximately three times higher than the level of baseline noise for each neuron. In addition, each file was manually inspected to reject spurious events caused by excessive noise and to include any events that were not detected by the program. All events with a 10 to 90% rise time of less than 5 ms were used in the analysis. The peak amplitude, 10 to 90% rise time, charge transfer (Q), and the time constant of current decay (τ_{decay}) were analyzed. Peak amplitude refers to the maximum height of the mIPSC, and rise time refers to the time elapsed between 10

and 90% of the peak amplitude response. All events recorded from each cell under each experimental condition were averaged to generate the average mIPSC for each neuron. The τ_{decay} was determined using the biexponential equation $I(t) = A_1\exp(-t/\tau_1) + A_2\exp(-t/\tau_2)$ where I is the current amplitude at any given time (t), A_1 and A_2 are the amplitudes of the fast and slow decay components, respectively, and τ_1 and τ_2 are their respective decay time constants. The weighted time constant ($\tau_{weighted}$) of current decay was determined using the equation $\tau_{weighted} = (A_1\tau_1 + A_2\tau_2)/(A_1 + A_2)$, and Q was determined by integrating the area under the average mIPSC.

Immunocytochemistry. The surface expression of GlyRs was studied using native receptors and recombinant receptors of known composition expressed in HEK 293 cells. In the cultures of spinal cord cells, neurons were incubated directly with the primary antibody (rabbit polyclonal to GlyR α_1, 1:10 dilution; Abcam Limited, Cambridge, UK) in neurobasal MEM containing 2 mg/ml phosphate-buffered saline (PBS) for 30 min at 37°C in an incubator containing 5.5% CO_2. After repeated washing with bovine serum albumin, cultures were fixed with 4% paraformaldehyde in PBS for 10 min and subsequently incubated with the secondary antibody (Alexa Fluor 488 goat anti-rabbit, 1:700 dilution).

The c-myc tag was introduced so that α_1 GlyRs could be stained and visualized using confocal microscopy. The c-myc epitope was inserted after the second amino acid of the extracellular C terminus of the GlyR α_1 subunit cDNA (QuikChange site-directed mutagenesis kit; Stratagene, La Jolla, CA). Twenty-four hours after HEK 293 cells were transfected with GlyR α_1 c-myc/pBK-CMV NB-200, the cells were fixed with 4% paraformaldehyde in PBS for 10 min under nonpermeabilizing conditions. Cells were washed in PBS, blocked in 4% bovine serum albumin, and primary antibody was applied (mouse monoclonal anti-c-myc, 1:10 dilution; Sigma-Aldrich) followed by a secondary antibody (Alexa Fluor 488 goat anti-mouse, 1:700 dilution; Invitrogen).

To test the effect of insulin on GlyR surface expression, some cultures were treated with insulin (1 μM) or vehicle control for 1 or 5 min before fixation (HEK 293 cells) or before incubation with primary antibody (cultured spinal cord cells). Immunostaining was visualized with a laser-scanning confocal microscope (Leica TCS SL; Leica Microsystem Heidelberg GmbH, Heidelberg, Germany). All cultures were imaged using identical confocal settings at maximum projection throughout all optical sections using Leica Confocal Software (Leica Microsystem Heidelberg GmbH) functions. Total surface fluorescence intensity was quantified using Scion Image software (beta ver. 4.03; Scion Corporation, Frederick, MD).

Data Analysis and Statistical Tests. Currents were recorded and analyzed with pCLAMP6 software (Molecular Devices, Sunnyvale, CA). Currents were normalized to the amplitude of control responses. The glycine concentration-response plot was fitted to the modified Michaelis-Menten equation: $I = I_{max}/[1 + (d/EC_{50})^{nH}]$, where I is the current amplitude, d is the agonist concentration, EC_{50} is the concentration of agonist that produces currents with amplitude of 50% of maximal response, and n_H is the estimated Hill coefficient. Data from paired and unpaired samples were used to generate the concentration-response plot. The reversal potential for Cl^- was calculated with the Nernst equation: $E_{Cl^-} = 58 \log [Cl^-]_{inside}/[Cl^-]_{outside}$. The amplitude of the peak current evoked by glycine was analyzed for all experiments except for those used to study the effects of HNMPA. Cumulative distribution plots of mIPSC amplitudes, charge transfer, and decay times were generated in GraphPad Prism 4 (GraphPad Software Inc., San Diego, CA) and analyzed using the Kolmogorov-Smirnov test. Data are expressed as mean ± S.E.M., and statistical analyses were performed with Student's t test, the Wilcoxon test, or one- or two-way analysis of variance, as appropriate. A p value of less than 0.05 was considered significant.

Results

Insulin Increases the Function of GlyRs in Spinal Neurons. Currents were evoked by applying a subsaturating concentration of glycine (15 μM) (Caraiscos et al., 2002) to spinal neurons in the absence and presence of various concentrations of insulin. Insulin was preapplied for 30 s and then coapplied with glycine for 2 s. The time interval between glycine applications was 1 min. Insulin caused a concentration-dependent increase in the amplitude of glycine-evoked current (I_{Gly}) as shown in Fig. 1. The threshold concentration of insulin that increased I_{Gly} was 1 μM. The insulin concentration that produced currents with amplitude of 50% of maximal response (EC_{50}) was 3.0 ± 1.0 μM and the Hill coefficient was 1.4 ± 0.2. (n = 8; Fig. 1, A and B). Heat-inactivated insulin (1 μM) failed to enhance current evoked by glycine (99 ± 3% of control, n = 5). Insulin (1 μM) applied alone in the absence of glycine did not generate a current because the holding current remained unchanged (104 ± 1% of control, n = 6). Coapplication experiments indicated that the onset of insulin enhancement of I_{Gly} was rapid because it occurred within the time scale of the perfusion system (approximately 3 ms). Enhancement of I_{Gly} was similar whether insulin was preapplied for 60 s or coapplied with glycine (139 ± 5% of control, n = 16, $p < 0.05$, and 143 ± 7% of control, n = 7, $p < 0.05$, respectively; Fig. 1C). Recovery from the insulin effect was studied by pretreating neurons with insulin (1 μM) for 5 min then applying an insulin-free extracellular solution. Within 1 min of insulin washout, the glycine current had an amplitude that was similar to control (107 ± 3% of control, n = 10; Fig. 1D). Ten minutes after washout, insulin was reapplied, and I_{Gly} was enhanced to 140 ± 10% of control (n = 7, $p < 0.05$). Thus, insulin caused a rapid, reversible, and reproducible increase in I_{Gly}.

Next, to determine whether insulin altered the equilibrium potential for chloride ions, the effect of insulin on the current-voltage relationship for I_{Gly} was examined. Insulin (1 μM) increased the slope conductance (15 ± 2 nS for control versus 21 ± 4 nS for insulin, n = 4, $p < 0.05$) but did not change the reversal potential, which was similar to the Nernst potential for chloride ions (approximately −16 mV) (Fig. 1, E and F). Enhancement of GlyRs by insulin occurred at both hyperpolarizing and depolarizing membrane potentials.

Insulin Increases the Potency of Glycine in Spinal Neurons. Enhancement of I_{Gly} by insulin could result from either direct potentiation of GlyRs or recruitment of new functional receptors to the plasma membrane or a combination of these effects. We predicted that if the number of functional receptors increased, the current activated by a saturating concentration of glycine would increase, as has been observed for $GABA_A$ receptors (Wan et al., 1997). Current activated by a saturating concentration of glycine (1 mM) was not enhanced by insulin (1 μM) (n = 5; Fig. 2, A and B), whereas current evoked by subsaturating concentrations of glycine was consistently increased. To determine whether the modulation of GlyRs by insulin resulted from an increase in the potency of glycine, concentration-response curves were constructed. Insulin (1 μM) shifted the concentration-response plot for I_{Gly} to the left and reduced the glycine EC_{50} value 1.7-fold from 52 ± 6 μM (n = 5) to 31 ± 2 μM (n = 5), $p < 0.05$ (Fig. 2, C and D). The n_H value was unchanged (1.5 ± 0.1 for control versus 1.6 ± 0.1 for insulin). These

results are consistent with the hypothesis that insulin increases the function of GlyRs by increasing the sensitivity to glycine.

Insulin Enhancement of Peak I_{Gly} Is Not Mediated by Contaminating Zinc. Commercial preparations of insulin are known to contain trace amounts of the divalent cation zinc (Zn^{2+}). The concentration of Zn^{2+} in commercial insulin solution is reported to range from 0.25 to 0.5 μM (from correspondence with Sigma-Aldrich). Low concentrations of Zn^{2+} (20 nM to 10 μM) potentiate I_{Gly} in spinal neurons, with maximal enhancement observed at approximately 1 μM, whereas higher concentrations of Zn^{2+} (approximately 20–50 μM) inhibit the function of GlyRs and reduce I_{Gly} (Lynch, 2004). Others have reported that Zn^{2+} at 1 μM increases agonist potency by decreasing dissociation, whereas Zn^{2+} at 100 μM decreases glycine potency (Laube et al., 1995). Synaptic Zn^{2+} is essential for proper in vivo functioning of glycinergic synaptic transmission (Hirzel et al., 2006). To determine whether trace levels of Zn^{2+} accounted for or contributed to insulin enhancement of I_{Gly}, two strategies were used. First, we observed that Zn^{2+} (1 μM) added to the extracellular solution increased I_{Gly} to 188 ± 18% of control (n = 10). The additional Zn^{2+} did not occlude the actions of insulin (1 μM) as insulin increased I_{Gly} to 132 ± 6% of control, n = 10, $p < 0.05$. Furthermore, increasing the Zn^{2+} concentration to 50 μM depressed I_{Gly} by 43 ± 9% of control (n = 6) but did not prevent insulin (1 μM) enhancement of the current (116 ± 5% of control, n = 6, $p < 0.05$). Next, because very low concentrations of Zn^{2+} are reported to not influence GlyR function, any possible contaminating level of Zn^{2+} was

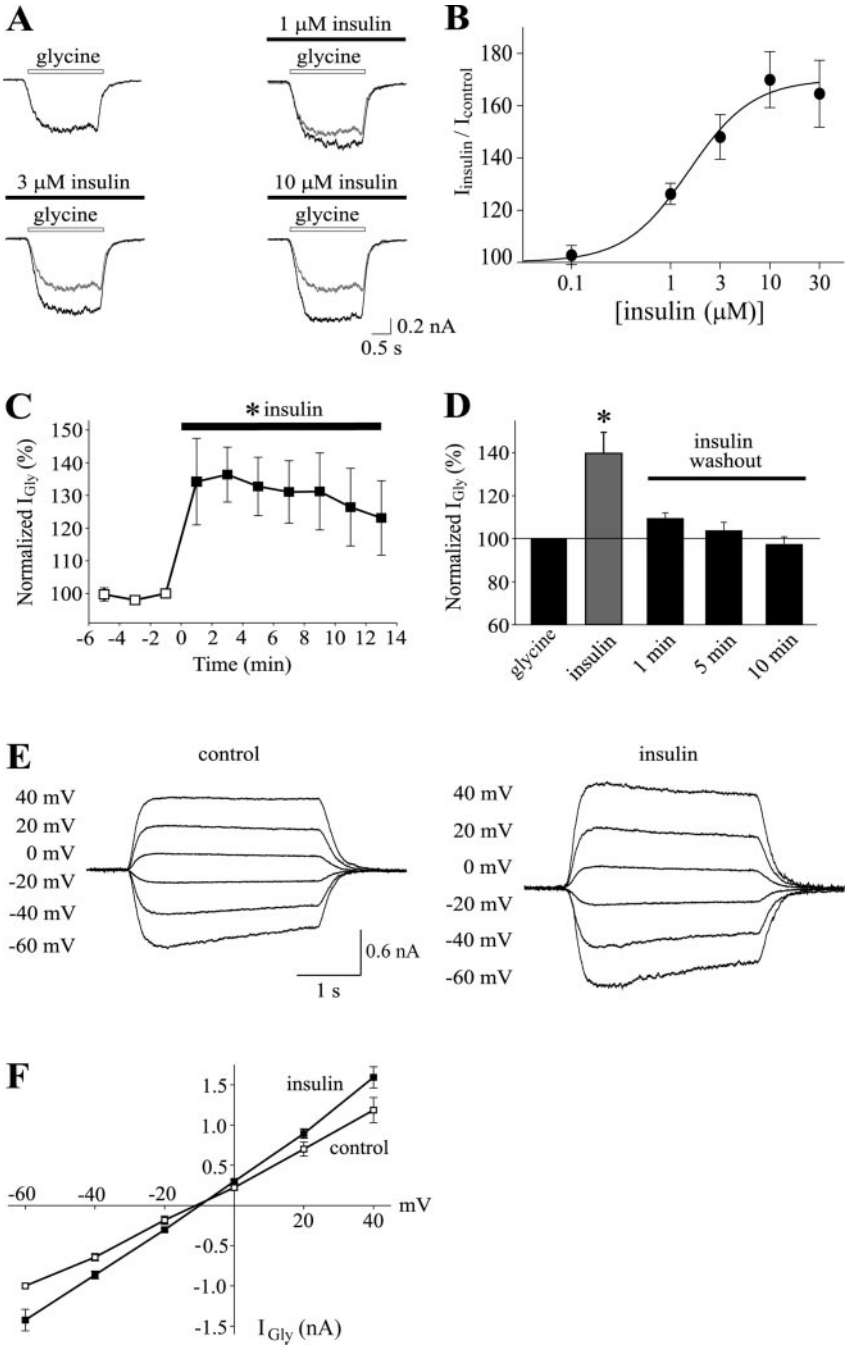

Fig. 1. Insulin increases the function of GlyRs in spinal neurons. A, currents evoked by glycine in the absence and presence of increasing concentrations of insulin are shown. B, concentration-response curve showing the insulin-mediated potentiation of current evoked by 15 μM glycine (n = 8). The x-axis shows the log concentration of insulin (in micromolar concentrations), and the y-axis represents I_{Gly} normalized to the maximum control response. C, plot showing the rapid onset of insulin (1 μM) enhancement of current activated by 15 μM glycine (n = 5). The maximal effect of insulin was observed by 1 min after coapplication of glycine and was sustained throughout the recording period of 13 min (*, $p < 0.05$). Several data points have error bars that are too small to see. D, bar graph summarizing the effect of insulin pretreatment on I_{Gly}. Neurons were pretreated with insulin (1 μM) for a period of 5 min, and currents evoked by glycine (15 μM) were recorded at 1 min (n = 10), 5 min (n = 7), and 10 min (n = 7) after insulin washout. Subsequent coapplication of insulin (1 μM) and glycine (15 μM) increased I_{Gly} in spinal neurons (n = 7;*, $p < 0.05$). E, control and insulin (1 μM)-enhanced currents evoked by glycine (15 μM), recorded at various membrane potentials. F, current-voltage relations of control (□) and insulin-enhanced (■) I_{Gly} (n = 4). All values were normalized to I_{Gly} activated by 15 μM glycine at −60 mV before the application of 1 μM insulin (*, $p < 0.05$).

further reduced to approximately 1 to 2 nM by adding the Zn^{2+} chelator tricine (10 mM) to the extracellular solution. Tricine alone reduced I_{Gly} to 57 ± 4% of control ($n = 4$, $p < 0.05$). Application of insulin (1 μM) in the presence of tricine enhanced I_{Gly} to 125 ± 4% of control ($n = 4$, $p < 0.05$). Together, these results indicate that insulin enhancement of I_{Gly} was independent of contamination by Zn^{2+}.

We also examined the effect of insulin on I_{Gly} recorded from neurons that had been grown in insulin-free media. Neurons grown in insulin-free media did not seem as healthy as controls because cell density and lifespan were lower than those of controls. The increase in I_{Gly} by insulin with tricine in the extracellular solution (125 ± 7% of control, $p < 0.05$, $n = 3$) was not different for neurons grown in insulin-free media.

The α Subunit Is Sufficient for Insulin Enhancement of I_{Gly}. Insulin modulation of several transmitter-gated ion channels depends on the subunit composition of the underlying receptors. For example, insulin potentiates NMDA receptors in a subunit-specific manner through signaling pathways involving PKCs (Jones and Leonard, 2005). Likewise, enhancement of $GABA_A$ receptors by insulin depends on the subunit complement of the receptors and involves tyrosine kinase-dependent pathways (Wan et al., 1997). We reported previously that tyrosine kinases up-regulate I_{Gly} by mechanisms that require the β subunit (Caraiscos et al., 2002). Thus, we tested the hypothesis that enhancement of I_{Gly} by insulin involves second-messenger systems that require the β subunit. In addition, because the subunit composition of native GlyRs in cultured spinal neurons is unknown, we sought to determine whether the adult α_1 isoform is sensitive to insulin.

To confirm the coexpression of α_1 and β subunits in HEK 293 cells, we first examined the sensitivity of I_{Gly} to picrotoxin as described previously (Caraiscos et al., 2002). Coexpression of the β subunit reduces the sensitivity of I_{Gly} to inhibition by picrotoxin (Lynch, 2004). Picrotoxin (1 mM) caused a greater inhibition of current generated by α_1 GlyRs (to 29 ± 13% of control, $n = 5$) compared with current generated by $\alpha_1\beta$ GlyRs (to 71 ± 4% of control, $n = 6$), consistent with the formation of heteromeric GlyRs. A glycine concen-

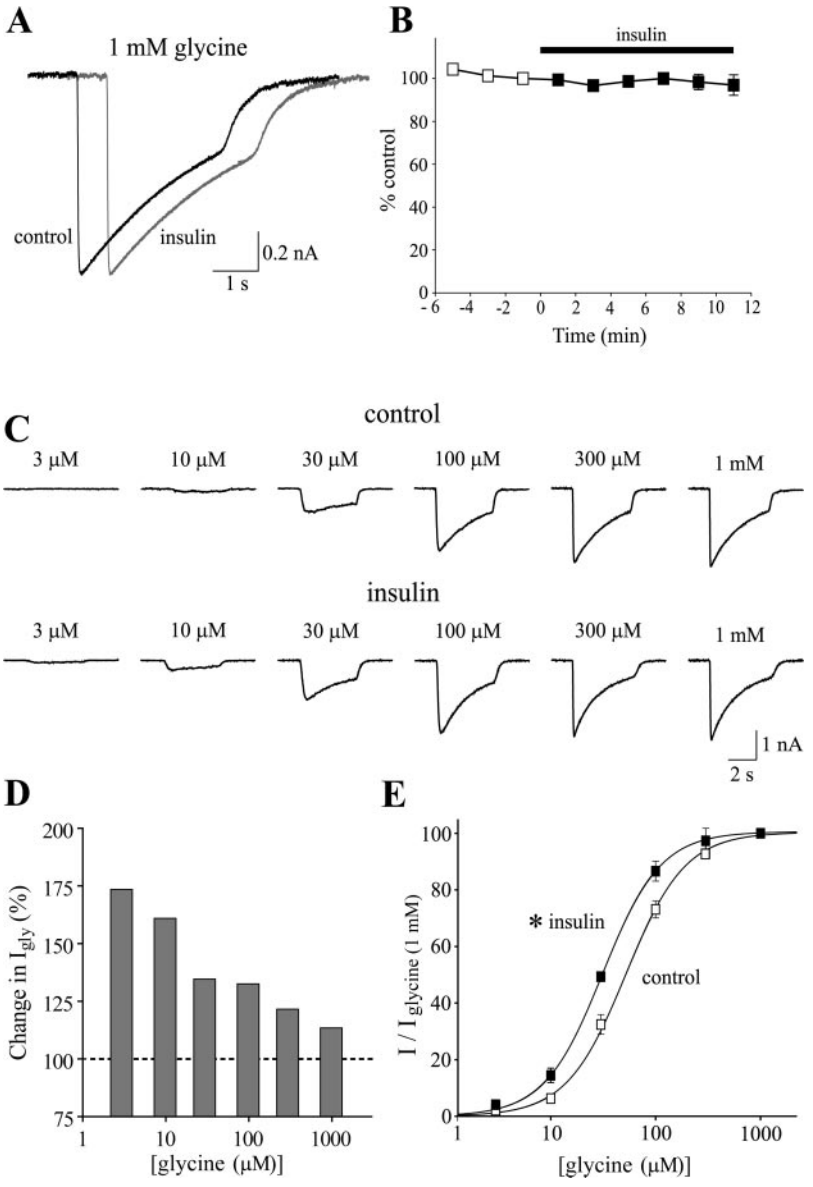

Fig. 2. Insulin increases the potency of glycine in spinal neurons. A, representative traces evoked by saturating glycine (1 mM) in the absence and presence of insulin (1 μM). B, plot illustrating the inability of insulin (1 μM) to potentiate currents evoked by 1 mM glycine ($n = 5$). C, representative traces evoked by glycine (3 μM to 1 mM) before and during the application of insulin (1 μM). D, the percentage of change in I_{Gly} induced by insulin at various concentrations of glycine for the recording shown in C. E, glycine concentration-response plots before ($n = 5$) and during ($n = 5$) application of insulin (1 μM). All values were normalized to the maximal I_{Gly} recorded when glycine (1 mM) was applied (*, $p < 0.05$ for comparison between control and insulin-treated groups).

tration of 100 μM was selected for these experiments because this subsaturating concentration approximates the EC_{50} values for α_1 (EC_{50} = 75 μM) and $\alpha_1\beta$ (EC_{50} = 55 μM) (Pribilla et al., 1992). Insulin (1 μM) increased the current generated by both α_1 homomeric and $\alpha_1\beta$ heteromeric GlyRs (118 ± 4% of control, n = 7, $p < 0.05$ and 120 ± 4% of control, n = 14, $p < 0.05$, respectively; Fig. 3). Hence, the β subunit is not required for the insulin enhancement of GlyRs, and homomeric α_1 GlyRs are sensitive to insulin.

Insulin Potentiation of I_{Gly} Is Mediated by the Insulin Receptor. To determine whether activation of the insulin receptor is required for the effects of insulin on I_{Gly}, we applied a compound that inhibits insulin receptor function. The membrane-permeable inhibitor HNMPA antagonizes both activity and autophosphorylation of insulin receptor tyrosine kinase (Saperstein et al., 1989). The concentrations of HNMPA that produce 50% of the maximum possible inhibitory response (IC_{50}) for insulin receptor activation and autophosphorylation are approximately 100 and 200 μM, respectively (Saperstein et al., 1989). To examine the effects of HNMPA and insulin in the same cell, the experimental protocol was slightly modified. We recorded currents activated by glycine (15 μM) that peaked and then decayed to a quasi-steady-state amplitude over 5 s as shown in Fig. 5. Insulin (1 μM), HNMPA (100 μM), or HNMPA (100 μM) plus insulin (1 μM) were coapplied with glycine for 5 s during the steady-state period (Fig. 4A). Insulin alone increased I_{Gly} (129 ± 6% of control, n = 5, $p < 0.05$) (Fig. 4B), whereas HNMPA alone did not alter the steady-state current evoked by glycine (99 ± 1% of control; Fig. 4, A and B). In another experiment, neurons were pretreated for 5 min with HNMPA (100 μM), and then HNMPA and insulin (1 μM) were coapplied. Under these conditions, HNMPA completely inhibited enhancement of I_{Gly} by insulin (102 ± 4% of control, n = 5; Fig. 4, A and B). Together, the results show that enhancement of I_{Gly} requires activation of the insulin receptor.

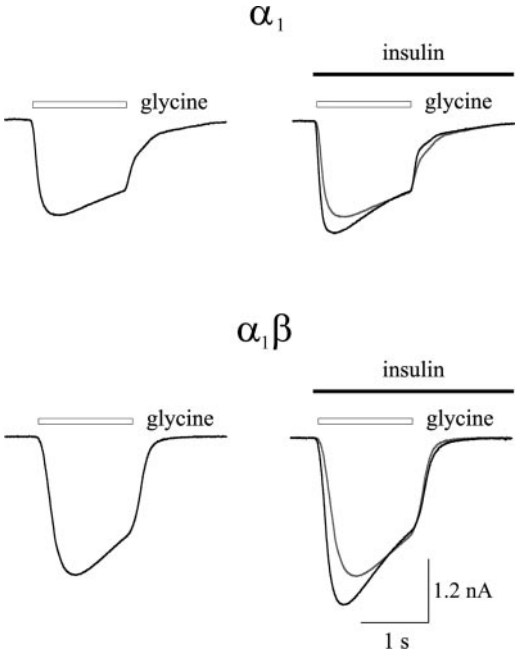

Fig. 3. Insulin enhancement of peak I_{Gly} is independent of the β subunit in HEK 293 cells. Traces of current evoked by glycine (100 μM) and mediated by α_1 and $\alpha_1\beta$ GlyRs expressed in HEK 293 cells before and during the application of insulin (1 μM) are shown.

Insulin Potentiation of I_{Gly} Involves PI3 Kinase and Tyrosine Kinases. The insulin receptor is a member of the superfamily of receptor tyrosine kinases. It is a dimer composed of two extracellular α subunits and two transmembrane β domains (De Meyts et al., 2004), in which the α subunit contains the ligand binding domain and the β subunit contains the tyrosine kinase sites. Binding of insulin to the insulin receptor activates signaling cascades that involve tyrosine kinases and PI3 kinases. We next sought to identify the cytosolic substrates that might be involved in insulin-GlyR signaling pathways. First, to determine whether tyrosine kinases contribute to the insulin enhancement of I_{Gly}, the effects of the tyrosine kinase inhibitor lavendustin A (10 μM) and its inactive analog lavendustin B (10 μM) were examined in spinal neurons. We reported previously that lavendustin A and lavendustin B cause a rapid, reversible, direct inhibition of GlyRs by approximately 35%, which is independent of actions on tyrosine kinases (Caraiscos et al., 2002). Lavendustin A caused a further 40% decrease in I_{Gly} in spinal neurons compared with lavendustin B via mechanisms involving tyrosine kinases (Caraiscos et al., 2002). In the present experiments, glycine was repeatedly applied until the currents stabilized in the presence of either lavendustin A or lavendustin B. Insulin was applied subsequently, and the change in I_{Gly} was measured. The inactive analog lavendustin B (10 μM) had no effect on insulin enhancement of I_{Gly} as the current was increased to 137 ± 7% of control (n = 7; $p < 0.05$). In contrast, lavendustin A completely abolished the enhancement of I_{Gly} by insulin (98 ± 4% of control, n = 7; Fig. 4, C and D). These results indicate that tyrosine kinases are involved in the pathways that mediate insulin-induced enhancement of I_{Gly} in spinal neurons. Because DMSO was used to dissolve lavendustin A and lavendustin B, the effects of extracellular DMSO alone on insulin-enhancement of glycine currents were examined. DMSO (0.1%) did not alter current evoked by glycine alone (101 ± 4% of control, n = 4). Furthermore, the enhancement of glycine-evoked current by insulin with DMSO in the extracellular solution (141 ± 7% of control, n = 5, $P > 0.05$) was similar to control.

To determine whether PI3 kinase was involved in the insulin potentiation of I_{Gly}, the PI3 kinase inhibitor wortmannin was added to the pipette solution. A low concentration of wortmannin (50 nM) was selected because higher concentrations inhibit other members of the PI3 kinase superfamily. Wortmannin (50 nM) applied in the absence of insulin had no effect on I_{Gly} but caused a time-dependent reduction of I_{Gly} enhanced by insulin (1 μM) (n = 7, $p < 0.05$; Fig. 5). The addition of the vehicle, DMSO (0.1%), alone to the intracellular fluid did not alter insulin enhancement of glycine current (146 ± 7%, n = 4, $p > 0.05$ compared with control). Thus, a PI3 kinase pathway is probably involved in the insulin-induced enhancement of GlyR function.

Gramicidin Perforated Patch Recordings. Under our recording conditions, the intracellular solution (in the electrode) contained a high concentration of chloride ions, which has been shown to influence intracellular signaling pathways (Lenz et al., 1997). In addition, the conventional whole-cell patch configuration alters cytosolic constituents of signaling

pathways and calcium buffering systems. To determine whether changes in the intracellular concentration of chloride ions or dilution of cytosolic substrates influenced the actions of insulin on I_{Gly}, we performed perforated patch recording using the gramicidin technique (Akaike, 1996). The increase in I_{Gly} by insulin (1 μM) was similar for currents recorded using whole-cell and gramicidin-perforated patch techniques (143 ± 7% of control, $n = 7$ versus 147 ± 15% of control, $n = 6$, respectively, $p > 0.05$). Thus, dialysis of intracellular constituents and disruption of the physiological chloride ion gradient did not alter insulin modulation of GlyR function.

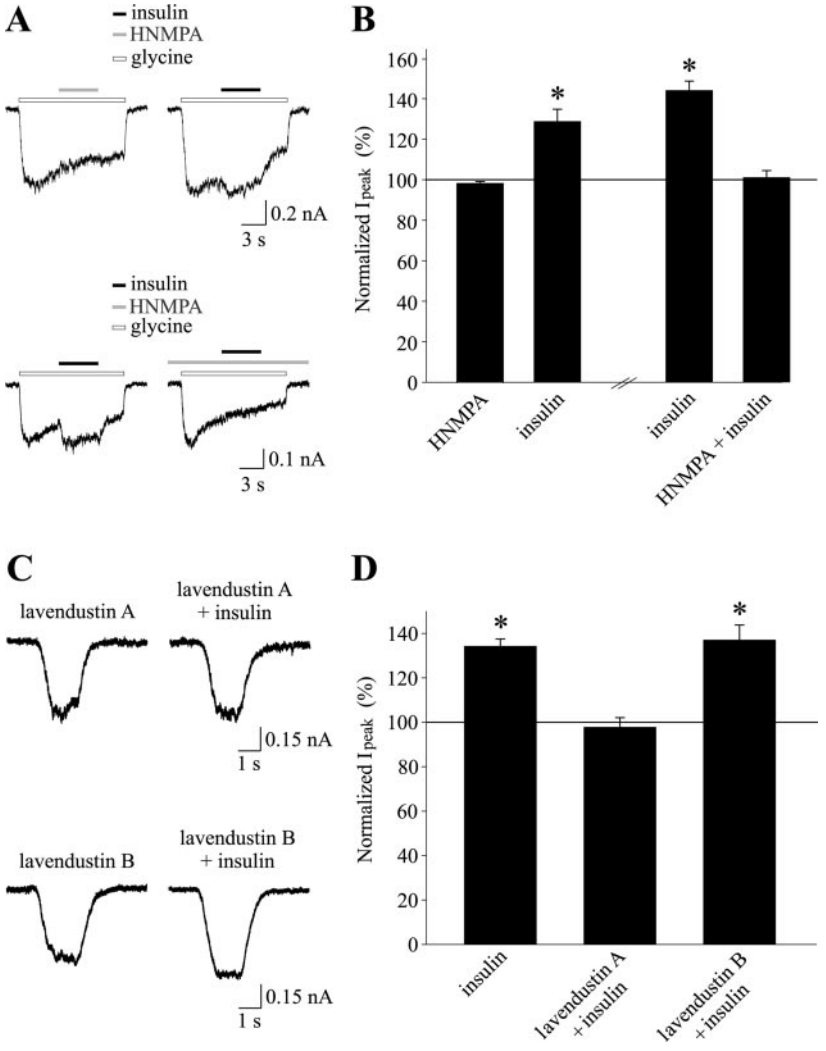

Fig. 4. Insulin potentiation of I_{Gly} is mediated by tyrosine kinases in spinal neurons. A, representative traces showing the effect of brief applications of HNMPA (100 μM) or insulin (1 μM) on currents evoked by 15 μM glycine in the same neuron. Glycine was applied alone for 5 s followed by coapplication of HNMPA or insulin and glycine (5 s) and then glycine alone (3 s). B, summary of the effects of HNMPA (100 μM) and insulin (1 μM) on I_{Gly} when applied in the same cell ($n = 5$), and the effect of insulin (1 μM) followed by coapplication of HNMPA and insulin on I_{Gly} ($n = 5$) (*, $p < 0.05$ for comparison between the control and HNMPA-treated group). C, the traces show that lavendustin A (10 μM) but not lavendustin B (10 μM) inhibits insulin enhancement of current evoked by glycine. D, plot summarizing the inhibitory effects of lavendustin A ($n = 7$) but not lavendustin B ($n = 7$) on the enhancement of I_{Gly} by insulin (1 μM) (*, $p < 0.05$ for comparison between control and treated groups).

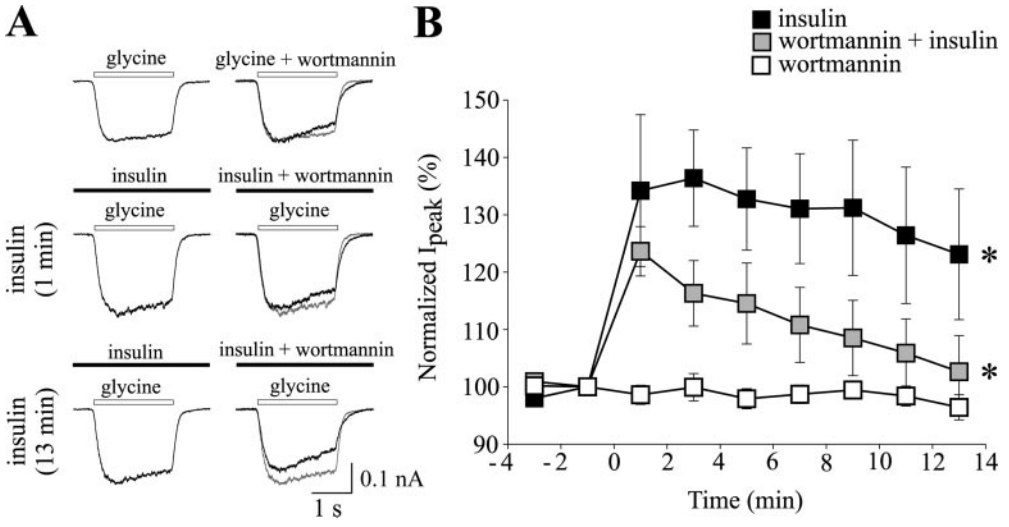

Fig. 5. Insulin potentiation of I_{Gly} is mediated by PI3 kinase in spinal neurons. A, currents evoked by glycine (15 μM) were recorded in the absence and presence of wortmannin (50 nM). Traces recorded before and during the application of insulin for 1 min and 13 min are shown. No significant change in current amplitude occurred over the 13 min. B, plot showing the effect of insulin (1 μM) on currents activated by 15 μM glycine in the absence (■, $n = 5$) and presence (■, $n = 7$) of wortmannin (50 nM) in the intracellular solution. Wortmannin (50 nM) did not affect control I_{Gly} (□, $n = 6$) in spinal neurons (*, $p < 0.05$ for comparison between control and treated groups).

Insulin Increases Inhibitory Glycinergic Synaptic Transmission in Spinal Neurons. To examine the effects of insulin on glycinergic synaptic transmission, spontaneous mIPSCs were recorded from cultured spinal neurons in the presence of ionotropic glutamate receptor antagonists and $GABA_A$ receptor antagonists. At least eight different sets of cultures were used for these experiments, and each culture dish was used to record from only one cell. Insulin (1 μM) increased the amplitude of mIPSCs to 124 ± 4% of control (38.9 ± 7.4 pA for control and 47.4 ± 8.8 pA for insulin, $n = 8$, $p < 0.05$; Fig. 6). Insulin also increased the charge transfer of mIPSCs to 135 ± 8% of control (507 ± 111 pA/ms for control and 706 ± 184 pA/ms for insulin, $n = 8$, $p < 0.05$). Insulin did not change the interspike time interval (11.5 ± 1.5 ms for control and 11.3 ± 1.8 ms for insulin), rise time (10–90%: 1.3 ± 0.2 ms for control and 1.3 ± 0.1 ms for insulin) or decay time (11.5 ± 1.5 ms for control and 11.3 ± 1.81 ms for insulin). The GlyR antagonist strychnine (1 μM) abolished the insulin-sensitive mIPSCs ($n = 5$; Fig. 6), confirming that the currents were generated by GlyRs.

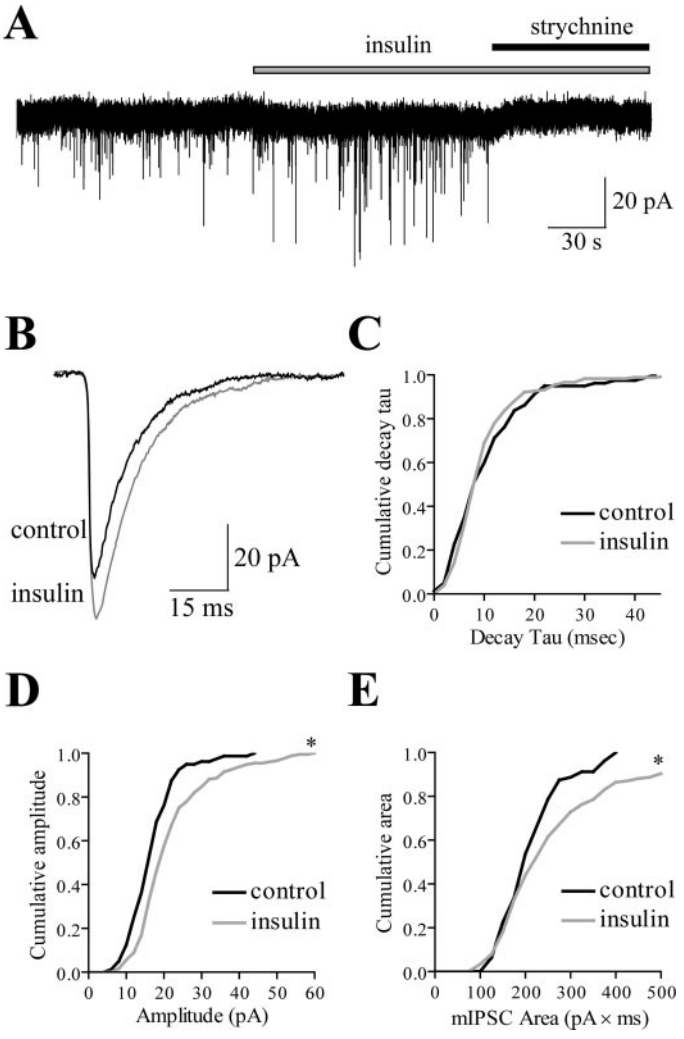

Fig. 6. Insulin increases inhibitory glycinergic synaptic transmission in spinal neurons. A, representative traces of currents recorded from spinal neurons in the absence and presence of insulin (1 μM) and strychnine (10 μM). Note that insulin increased the amplitude of mIPSCs whereas strychnine abolished the mIPSCs and shifted the baseline upward, possibly caused by inhibition of a tonic glycinergic current. B, representative averaged traces of glycinergic mIPSCs before and during the bath application of insulin (1 μM). Insulin increased the mean amplitude and charge transfer of mIPSCs. C, D, and E, cumulative distribution plots illustrate the increase by insulin of the current amplitude and charge transfer of glycinergic mIPSCs recorded in a spinal neuron (*, $p < 0.05$).

We next sought to determine whether a tonic glycinergic current is generated by cultured spinal neurons. The tonic glycinergic current was detected by applying strychnine (1 μM) and measuring the change in the holding current. Strychnine (1 μM) failed to reduce the holding current (0.45 ± 1.3 pA, $n = 7$, $p > 0.05$) indicating the absence of a tonic glycinergic current. Consistent with this result, the application of insulin alone failed to alter the holding current (104% of control as reported above). Thus, insulin increases synaptic but not tonic glycinergic currents in cultured spinal neurons.

Insulin Does Not Affect GlyR Surface Expression in HEK 293 Cells and Spinal Neurons. The above results are consistent with insulin causing an increase in the function of GlyRs rather than an increase in the number of functional GlyRs expressed at the plasma membrane. However, insulin has been shown previously to stimulate the recruitment of functional $GABA_A$ and NMDA receptors to the plasma membrane (Wan et al., 1997; Skeberdis et al., 2001). It is possible that insulin also increased the surface expression of GlyRs, but they remained inactive. To examine the effects of insulin on the expression of GlyRs, immunocytochemistry was used to visualize human recombinant c-myc-tagged GlyRs expressed in HEK 293 cells and native GlyRs in spinal neurons. First, to ensure that the c-myc epitope did not affect receptor function, we recorded whole-cell current generated by GlyRs containing c-myc-tagged-α_1 subunits and the β subunit. The maximal current (I_{max}) generated by $\alpha_1\beta$ GlyRs and c-myc-tagged-$\alpha_1\beta$ GlyRs was similar (I_{max} = 2194 ± 366 pA, $n = 14$, and 1738 ± 672 pA, $n = 7$, respectively, $p > 0.05$).

Immunostaining against c-myc-tagged-α_1 expressed in HEK 293 cells showed that incubation with insulin (1 μM) for 1 or 5 min did not alter the amount of surface fluorescence intensity relative to control (Fig. 7, A and B). We also examined the surface expression of native GlyRs in spinal neurons by immunostaining for the GlyR α_1 subunit. No change in fluorescence intensity was observed after the treatment of neurons with insulin (1 μM) for either 1 or 5 min relative to control (Fig. 7, C and D). Together, these results indicate that insulin does not change the number of functional GlyRs at the plasma membrane.

Discussion

Electrophysiological and immunochemical techniques were used to investigate the effects of insulin on GlyRs in spinal neurons and recombinant human GlyRs expressed in HEK 293 cells. The results showed that insulin caused a rapid and reversible increase in GlyR function. The potency of glycine was increased via mechanisms that involved, at least in part, the insulin receptor, PI3 kinase, and tyrosine kinases. The adult α1 subunit isoform was both sensitive and sufficient for insulin to induce an effect.

Insulin actions on GlyRs are fundamentally different from those that modify NMDA and $GABA_A$ receptors. Insulin enhancement of NMDA receptors results from the delivery of new channels to the cell membrane via soluble *N*-ethylmaleimide sensitive factor attachment receptor-dependent exocytosis (Wan et al., 1997; Skeberdis et al., 2001). Enhancement

of $GABA_A$ receptors in hippocampal neurons occurs via recruitment of new receptors to the cell membrane (Wan et al., 1997). These mechanisms contrast those that underlie insulin modulation of GlyRs because agonist potency rather than the number of functional GlyRs is increased. Despite such differences, insulin modulation of glycine, NMDA, and $GABA_A$ receptors share several common features. Carbachol enhancement of $GABA_A$ receptors in cortical pyramidal neurons only occurred when neurons were pretreated with insulin. This insulin-induced enhancement of $GABA_A$ receptors was dependent on PKC, protein tyrosine kinase Src-mediated signaling cascades, and PI3 kinase-dependent pathways (Ma et al., 2003). Insulin up-regulated postsynaptic $GABA_A$ receptors and increased the amplitude of spontaneous mIPSCs recorded in hippocampal CA1 neurons without altering the time course of mIPSC activation or decay (Wan et al., 1997). Likewise, we showed that insulin enhanced the amplitude but not the frequency of glycinergic mIPSCs in spinal neurons suggesting a postsynaptic rather than presynaptic site of action. Insulin potentiated NMDA receptor-mediated currents via activation of the insulin receptor tyrosine kinase because potentiation was eliminated by HNMPA (Skeberdis et al., 2001). It is interesting that a study of recombinant NMDA receptors that lacked all known sites of tyrosine and serine/threonine phosphorylation showed that insulin potentiation did not require direct phosphorylation of the NMDA receptor (Skeberdis et al., 2001). Insulin enhancement of GlyR function did not require the β subunit. Because the β subunit is required for up-regulation of GlyRs by the protein tyrosine kinase cSrc (Caraiscos et al., 2002), direct phosphorylation by Src does not contribute to insulin potentiation of GlyRs.

Insulin enhancement of GlyRs was mediated by pathways involving the insulin receptor and PI3 kinase. The cell signaling networks that are regulated by the insulin receptor are complex and contain multiple and divergent signaling cascades (Taniguchi et al., 2006). Insulin binding to its receptor causes phosphorylation of insulin receptor substrate proteins, which recruit the Src homology 2 domain-containing lipase kinase, PI3 kinase. PI3 kinase catalyzes phosphorylation of phosphoinositides on the 3-position to produce phosphatidylinositol (3,4,5) triphosphate (Reichardt, 2006). A variety of downstream second-messenger systems use phosphatidylinositol (3,4,5) triphosphate, including mitogen-activated protein kinase and stress-induced protein kinase. Growth factors and insulin may share similar actions on GlyRs because the activation of insulin-like-growth factor-1 (IGF-1) receptor rapidly (within seconds) increases the potency of taurine for GlyRs; however, the actions of IGF-1 were independent of PI3 kinase pathways because they are insensitive to wortmannin (Ster et al., 2005).

G protein-coupled receptors and receptor protein kinases regulate many of the same signaling molecules and molecular intermediates. G protein-coupled receptors can transactivate receptor tyrosine kinases (Ferguson, 2003); conversely, receptor tyrosine kinases can activate G protein-coupled receptors. For example, the receptor tyrosine kinase IGF-1 activates G proteins leading to G protein $\beta\gamma$ subunit-mediated Ras-dependent mitogen-activated protein kinase stimulation (Kuemmerle and Murthy, 2001). Such reciprocal interactions raise the intriguing possibility that G protein $\beta\gamma$ subunits participate in insulin modulation of GlyRs. Consistent with this notion, G protein-coupled receptors increase I_{Gly} in spinal cord neurons to approximately 160% of control

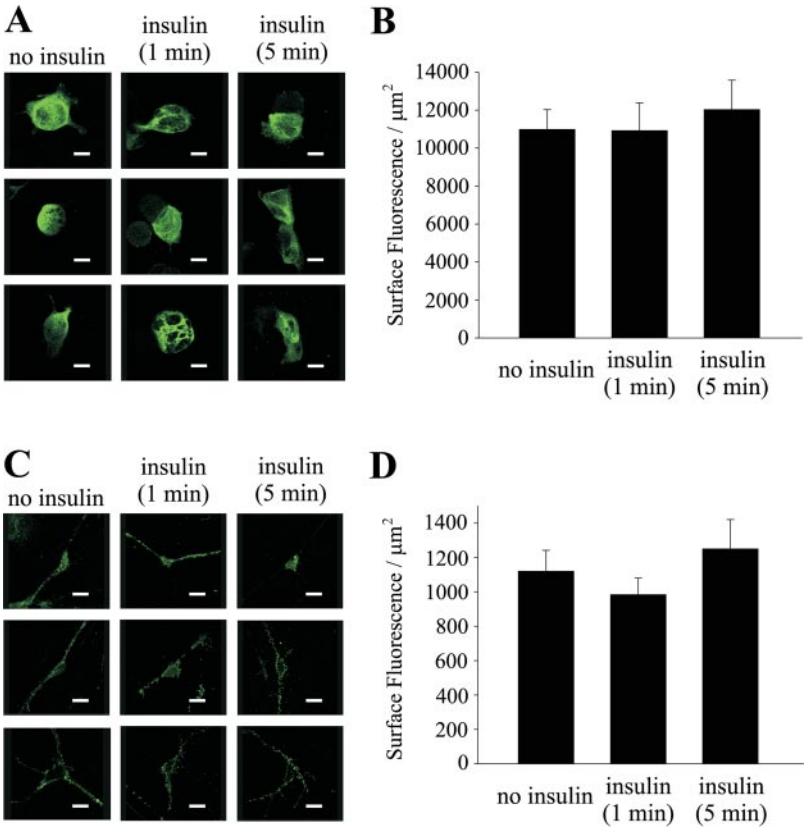

Fig. 7. Insulin does not affect GlyR surface expression in HEK 293 cells and spinal neurons. A, examples of HEK 293 cells expressing c-myc-tagged-α_1 GlyRs stained for the c-myc-tagged-α_1 subunit in the absence of insulin and after incubation with insulin (1 μM) for 1 or 5 min. Total surface fluorescence intensity is shown for each cell (scale bar = 8 μm). B, bar graph summarizing the total surface fluorescence intensity in the absence of insulin (n = 10) and after incubation with insulin (1 μM) for 1 (n = 10) or 5 min (n = 10). C, examples of spinal neurons stained for the GlyR α_1 subunit in the absence of insulin and after treatment with insulin (1 μM) for 1 or 5 min. Total surface fluorescence intensity for the GlyR α_1 subunit is shown for each cell (scale bar = 16 μm). D, bar graph summarizing the total surface fluorescence intensity for the GlyR α_1 subunit in spinal neurons in the absence of insulin (n = 14) and after treatment with insulin (1 μM) for 1 (n = 13) or 5 min (n = 15).

by increasing the potency of glycine (Yevenes et al., 2003). Glycine potency was increased 1.4-fold as the EC_{50} value decreased from 30 μM to 21 μM via phosphorylation-independent mechanisms involving G-protein $\beta\gamma$ subunits (Yevenes et al., 2003). The effects of overexpression of G protein $\beta\gamma$ subunits on GlyR function were examined using recombinant α_1 homomeric receptors expressed in HEK 293 cells. G protein $\beta\gamma$ overexpression potentiated I_{Gly} evoked by subsaturating concentrations of glycine and reduced the glycine EC_{50} value from 30 to 15 μM (Yevenes et al., 2003). Studies using mutant GlyRs showed that two basic amino acids within the large intracellular loop of the GlyR α_1 subunit are critical for the binding and functional modulation by G protein $\beta\gamma$ subunits (Yevenes et al., 2006).

We showed that insulin increased the potency of glycine for GlyRs 1.7-fold. An increase in agonist affinity would effectively up-regulate GlyRs that are activated by low or subsaturating concentrations of glycine. Extrasynaptic GlyRs that generate a nonsynaptic tonic glycinergic inhibition in several brain regions, including the hypothalamo-neurohypophyseal complex, cortex, and hippocampus, are believed to be activated by low ambient concentrations of glycine (Lynch, 2004). The tonic glycinergic inhibition generated in these regions may be enhanced by insulin. Cultured spinal neurons do not generate a tonic glycinergic conductance, possibly caused by either a low concentration of agonist or too few extrasynaptic GlyRs. This result is consistent with the absence of a tonic glycinergic current in the lamina II region of spinal cord in the adult mice (Ataka and Gu, 2006).

Insulin effects were studied primarily using embryonic, not mature, neurons. The complement of GlyR subunits in cultured spinal neurons is uncertain as the expression of subunits changes at various ontogenic stages and during postnatal development (Legendre, 2001; Aguayo et al., 2004). The α_1 subunit isoform is found mainly in adult spinal cord, brainstem, and colliculi of adult rodents, whereas the α_2 isoform is predominant in fetal and newborn neurons. The switch from the fetal α_2 isoform to the α_1 subunit occurs in the spinal neuron both in vivo and in vitro (Aguayo et al., 2004). The β subunit is widely distributed in the central nervous system, and GlyRs receptors change from α homomeric to $\alpha\beta$ heteromeric complexes with maturation. Different α subunit isoforms generally cause only subtle changes in the pharmacological properties between GlyRs; nevertheless, the complement of GlyR subunits in cultured spinal neurons studied is of interest. The relative abundance of α_2 and α_1 subunits in cultured spinal neurons has been studied using electrophysiology and reverse transcription-polymerase chain reaction analysis of mRNA (Aguayo et al., 2004). In rat spinal cord neurons prepared at 14 days of gestation and studied up to 10 DIV, the expression of α_1 subunit mRNA increased up to 3 DIV and then remained constant to 10 DIV. The α_2 subunit mRNA doubled from 1 to 5 DIV and then declined by 10 DIV to levels close to that observed at 1 DIV. Thus, the adult isoform of the GlyR probably contributes to the insulin-sensitive I_{Gly} in cultured spinal neurons.

The concentration of insulin in the brain is unknown but may be as high as 0.02 μM (Havrankova et al., 1978). The lowest concentration of insulin that increased I_{Gly} was 1 μM, suggesting that a pharmacological rather than a physiological concentration of insulin enhances I_{Gly}. However, it is plausible that GlyRs localized in proximity to insulin release sites may be exposed to high concentrations of insulin. Insulin has a wide spectrum of actions, and whether effects on GlyRs account for or contribute to the analgesic properties of insulin remains to be determined. Both GlyRs and insulin have been implicated in pain processes; however, this report provides the first evidence of an interaction between these two factors. The GlyR is the main inhibitory receptor in the spinal cord and brainstem; hence, insulin regulation of glycinergic activity may influence physiological processes regulated by these structures. Indeed, behavioral studies have showed that insulin influenced pain transduction at the level of the spinal cord (Courteix et al., 1996; Takeshita and Yamaguchi, 1997). Previous studies have implicated reduction in the function and/or number of GlyRs in neuropathic pain (Simpson et al., 1996; Simpson and Huang, 1998), allodynia (Yaksh, 1989; Sorkin and Puig, 1996), and hyperalgesia (Beyer et al., 1985, 1988), which suggests that glycinergic neurons may modulate afferent transmission relating to pain. Insulin acted as an analgesic agent in animal models because it attenuated formalin-induced nociceptive responses in normal mice, independent of plasma glucose levels (Takeshita and Yamaguchi, 1997). Furthermore, long-term insulin treatment relieved long-term hyperalgesia in mice with streptozocin-induced diabetes (Courteix et al., 1996) and exerted antinociception in both streptozotocin-induced diabetic mice and genetically diabetic db/db mice (Takeshita and Yamaguchi, 1997). As noted above, insulin also modifies other transmitter-gated ion channels that contribute to pain processes including α-amino-3-hydroxy-5-methylisoxazole-4-propionic acid, NMDA, and $GABA_A$ receptors. It remains to be determined how or whether insulin-enhancement of glycinergic inhibition integrates with other neurotransmitter systems in vivo to modify nociception. In summary, insulin has a novel regulatory action on GlyRs via mechanisms that are fundamentally different from insulin modulation of other transmitted-gated ion channels, including NMDA and $GABA_A$ receptors.

Acknowledgments

We thank Lidia Brandes and Waldemar Czerwinski for technical assistance and Dr. Wei-Yang Lu for his careful review of the manuscript.

References

Aguayo LG, van Zundert B, Tapia JC, Carrasco MA, and Alvarez FJ (2004) Changes on the properties of glycine receptors during neuronal development. *Brain Res Brain Res Rev* **47:**33–45.
Akaike N (1996) Gramicidin perforated patch recording and intracellular chloride activity in excitable cells. *Prog Biophys Mol Biol* **65:**251–264.
Ataka T and Gu JG (2006) Relationship between tonic inhibitory currents and phasic inhibitory activity in the spinal cord lamina II region of adult mice. *Mol Pain* **2:**36.
Beyer C, Banas C, Gomora P, and Komisaruk BR (1988) Prevention of the convulsant and hyperalgesic action of strychnine by intrathecal glycine and related amino acids. *Pharmacol Biochem Behav* **29:**73–78.
Beyer C, Roberts LA, and Komisaruk BR (1985) Hyperalgesia induced by altered glycinergic activity at the spinal cord. *Life Sci* **37:**875–882.
Caraiscos VB, Mihic SJ, MacDonald JF, and Orser BA (2002) Tyrosine kinases enhance the function of glycine receptors in rat hippocampal neurons and human alpha$_1$beta glycine receptors. *J Physiol* **539:**495–502.
Clarke DW, Mudd L, Boyd FT Jr, Fields M, and Raizada MK (1986) Insulin is released from rat brain neuronal cells in culture. *J Neurochem* **47:**831–836.
Courteix C, Bardin M, Massol J, Fialip J, Lavarenne J, and Eschalier A (1996) Daily insulin treatment relieves long-term hyperalgesia in streptozocin diabetic rats. *Neuroreport* **7:**1922–1924.
De Meyts P, Palsgaard J, Sajid W, Theede AM, and Aladdin H (2004) Structural biology of insulin and IGF-1 receptors. *Novartis Found Symp* **262:**160–171.
Ferguson SS (2003) Receptor tyrosine kinase transactivation: fine-tuning synaptic transmission. *Trends Neurosci* **26:**119–122.
Havrankova J, Schmechel D, Roth J, and Brownstein M (1978) Identification of insulin in rat brain. *Proc Natl Acad Sci USA* **75:**5737–5741.

Hirzel K, Muller U, Latal AT, Hulsmann S, Grudzinska J, Seeliger MW, Betz H, and Laube B (2006) Hyperekplexia phenotype of glycine receptor alpha1 subunit mutant mice identifies Zn^{2+} as an essential endogenous modulator of glycinergic neurotransmission. *Neuron* **52:**679–690.
Jones ML and Leonard JP (2005) PKC site mutations reveal differential modulation by insulin of NMDA receptors containing NR2A or NR2B subunits. *J Neurochem* **92:**1431–1438.
Kuemmerle JF and Murthy KS (2001) Coupling of the insulin-like growth factor-I receptor tyrosine kinase to G_{i2} in human intestinal smooth muscle: G$\beta\gamma$-dependent mitogen-activated protein kinase activation and growth. *J Biol Chem* **276:**7187–7194.
Laube B, Kuhse J, Rundstrom N, Kirsch J, Schmieden V, and Betz H (1995) Modulation by zinc ions of native rat and recombinant human inhibitory glycine receptors. *J Physiol* **483:**613–619.
Laube B, Maksay G, Schemm R, and Betz H (2002) Modulation of glycine receptor function: a novel approach for therapeutic intervention at inhibitory synapses? *Trends Pharmacol Sci* **23:**519–527.
Legendre P (2001) The glycinergic inhibitory synapse. *Cell Mol Life Sci* **58:**760–793.
Lenz RA, Pitler TA, and Alger BE (1997) High intracellular Cl^- concentrations depress G-protein-modulated ionic conductances. *J Neurosci* **17:**6133–6141.
Lynch JW (2004) Molecular structure and function of the glycine receptor chloride channel. *Physiol Rev* **84:**1051–1095.
Ma XH, Zhong P, Gu Z, Feng J, and Yan Z (2003) Muscarinic potentiation of $GABA_A$ receptor currents is gated by insulin signaling in the prefrontal cortex. *J Neurosci* **23:**1159–1168.
Park CR (2001) Cognitive effects of insulin in the central nervous system. *Neurosci Biobehav Rev* **25:**311–323.
Pribilla I, Takagi T, Langosch D, Bormann J, and Betz H (1992) The atypical M2 segment of the beta subunit confers picrotoxinin resistance to inhibitory glycine receptor channels. *EMBO (Eur Mol Biol Organ) J* **11:**4305–4311.
Reichardt LF (2006) Neurotrophin-regulated signalling pathways. *Philos Trans R Soc Lond B Biol Sci* **361:**1545–1564.
Saltiel AR and Pessin JE (2002) Insulin signaling pathways in time and space. *Trends Cell Biol* **12:**65–71.
Saperstein R, Vicario PP, Strout HV, Brady E, Slater EE, Greenlee WJ, Ondeyka DL, Patchett AA, and Hangauer DG (1989) Design of a selective insulin receptor tyrosine kinase inhibitor and its effect on glucose uptake and metabolism in intact cells. *Biochemistry* **28:**5694–5701.
Schulingkamp RJ, Pagano TC, Hung D, and Raffa RB (2000) Insulin receptors and insulin action in the brain: review and clinical implications. *Neurosci Biobehav Rev* **24:**855–872.
Simpson RK Jr, Gondo M, Robertson CS, and Goodman JC (1996) Reduction in the mechanonociceptive response by intrathecal administration of glycine and related compounds. *Neurochem Res* **21:**1221–1226.
Simpson RK Jr and Huang W (1998) Glycine receptor reduction within segmental gray matter in a rat model in neuropathic pain. *Neurol Res* **20:**161–168.
Skeberdis VA, Lan J, Zheng X, Zukin RS, and Bennett MV (2001) Insulin promotes rapid delivery of N-methyl-D-aspartate receptors to the cell surface by exocytosis. *Proc Natl Acad Sci USA* **98:**3561–3566.
Sorkin LS and Puig S (1996) Neuronal model of tactile allodynia produced by spinal strychnine: effects of excitatory amino acid receptor antagonists and a mu-opiate receptor agonist. *Pain* **68:**283–292.
Ster J, Colomer C, Monzo C, Duvoid-Guillou A, Moos F, Alonso G, and Hussy N (2005) Insulin-like growth factor-1 inhibits adult supraoptic neurons via complementary modulation of mechanoreceptors and glycine receptors. *J Neurosci* **25:**2267–2276.
Sugimoto K, Murakawa Y, and Sima AA (2002) Expression and localization of insulin receptor in rat dorsal root ganglion and spinal cord. *J Peripher Nerv Syst* **7:**44–53.
Takeshita N and Yamaguchi I (1997) Insulin attenuates formalin-induced nociceptive response in mice through a mechanism that is deranged by diabetes mellitus. *J Pharmacol Exp Ther* **281:**315–321.
Taniguchi CM, Emanuelli B, and Kahn CR (2006) Critical nodes in signalling pathways: insights into insulin action. *Nat Rev Mol Cell Biol* **7:**85–96.
Wan Q, Xiong ZG, Man HY, Ackerley CA, Braunton J, Lu WY, Becker LE, MacDonald JF, and Wang YT (1997) Recruitment of functional $GABA_A$ receptors to postsynaptic domains by insulin. *Nature (Lond)* **388:**686–690.
Xing Y, Sonner J, Laster MJ, Abaigar W, Caraiscos VB, Orser B, and Eger EI (2004) Insulin decreases isoflurane minimum alveolar anesthetic concentration in rats independently of an effect on the spinal cord. *Anesth Analg* **98:**1712–1717.
Yaksh TL (1989) Behavioral and autonomic correlates of the tactile evoked allodynia produced by spinal glycine inhibition: effects of modulatory receptor systems and excitatory amino acid antagonists. *Pain* **37:**111–123.
Yevenes GE, Moraga-Cid G, Guzman L, Haeger S, Oliveira L, Olate J, Schmalzing G, and Aguayo LG (2006) Molecular determinants for G protein $\beta\gamma$ modulation of ionotropic glycine receptors. *J Biol Chem* **281:**39300–39307.
Yevenes GE, Peoples RW, Tapia JC, Parodi J, Soto X, Olate J, and Aguayo LG (2003) Modulation of glycine-activated ion channel function by G-protein $\beta\gamma$ subunits. *Nat Neurosci* **6:**819–824.

Address correspondence to: Dr. Beverley A. Orser, The Department of Physiology, Room 3318, Medical Sciences Building, 1 King's College Circle, Toronto, Ontario, Canada, M5S1A8. E-mail: beverley.orser@utoronto.ca